



SCIREA Journal of Chemistry

<http://www.scirea.org/journal/Chemistry>

March 7, 2021

Volume 6, Issue 1, February 2021

## **Chiral Phases in a System of Biaxial Molecules II : Examining the Assembly of Rod-like Molecules**

**Masahito Hosino and Keisuke Ijuin**

Norikura 1-1303-2, Midori-ku, Nagoya 458-0004, Japan.

**Email:** [h08ubp53a1@hi3.enjoy.ne.jp](mailto:h08ubp53a1@hi3.enjoy.ne.jp)

### **Abstract**

One of the authors of the present study has already investigated chiral phases in a system of biaxial molecules based on the theory of biaxial liquid crystals, which we introduced in a previous work. In the earlier investigation, we assumed that the direction of the orientational ordering of the molecular long axis is perpendicular to the axis of the spiral structure. In this article, our premise is that this is not perpendicular to the axis of the spiral structure. In this assumption, the free energy of the system depends on the angle between the direction of the orientational ordering of the long axis and the axis of the spiral. The equilibrium value of this angle is determined based on the obtained free energy. As a result, we can show the presence of the cholesteric phase, new chiral phases, and the possible appearance of a twist-bend nematic phase.

**Keywords:** cholesteric phase, new chiral phases, twist-bend nematic phase

## 1. Introduction

Since the discovery of liquid crystals, all researchers in liquid crystals were thinking that the shape of their constituent molecules was rod-like one, despite their slightly biaxial shapes, and that this biaxiality did not affect properties of liquid crystals as their constituent molecules were rotating around their molecular long axis. The temperature dependence of cholesteric pitch was thought firstly as the phenomenon in which the molecular biaxiality results. It was thought that either the biaxiality of the molecular shape or the biaxial orientational orderings in the assembly of these molecules was one of three causes of the cholesteric pitch temperature dependence [1]. Although the temperature dependence of the cholesteric pitch was theoretically shown in the assembly of molecules with a hard repulsive core interacting via an attractive diversion force [2, 3], the effect of the molecular biaxiality on the cholesteric pitch temperature dependence has only recently been theoretically made clear [4].

Since the experimental discoveries of biaxial nematic [5 – 7] liquid crystals and the discotic [8 – 10] liquid crystals, it has become to be necessary that these liquid crystals should be theoretically discussed, basing on the assembly of biaxial molecules. In addition, the uniaxial phases, biaxial phases, and discotic phases appear in the assembly of molecules having rod-like shapes, and / or the anisotropy of the molecular interaction, plate-like shapes, and / or the anisotropy of the molecular interaction, and disc-like shapes, and / or the anisotropy of the molecular interaction, respectively. Thus, the relation between the shapes of the molecules and / or the anisotropies of the molecular interactions and the phases appear in the system of such molecules had to be clarified. Freiser [11] first proposed the model of the biaxial molecule and was able to show that the biaxial phase appeared at lower temperatures after the uniaxial phase. However, he could not explain the relationships described above.

After this, Straley [12] – by analogy with the intermolecular potential energy achieved as a repulsive forces, with a hard core between rectangular parallelepipeds with length  $L$ , breadth  $B$ , and depth  $D$  – proposed a molecular model where the intermolecular potential energy resulted from an attractive force interacting between pairs of molecules. He was able to describe the relationship between liquid crystal phases and the shapes of the molecule and / or the anisotropies of the molecular interaction composing their phases. In particular, his investigation showed the “self-dual” condition,  $B^2 = LD$ , which gives the boundary between the phases appearing in the assembly of rod-like molecules and those appearing in the

assembly of disc-like molecules. However, this theory was inconsistent as it is based on the intermolecular potential achieved through attractive forces between pairs of molecules, while the intermolecular potential strength parameters is determined by analogy with the intermolecular potential energy achieved through repulsive forces, with the hard core between rectangular parallelepipeds.

One of the present authors proposed that the intermolecular potential energy was the induced dipole-dipole interaction potential in the multipole expansion of the intermolecular potential energy of electrically neutral molecules, with three mutually orthogonal mirror planes with inversion symmetry [13]. This was similar to the molecular interaction potential energy proposed by Straley, except that it is physically consistent. Based on this molecular model, the relationship between the shapes of the molecule and / or the anisotropies of the molecular interaction and the phases observed could be explained, just as Straley did. The boundary condition between the phases appearing in the assembly of rod-like molecules and those appearing in the assembly of disc-like molecules was consistent with one shown in the investigation carried out by Sonnet et al. after the present authors' investigation [14].

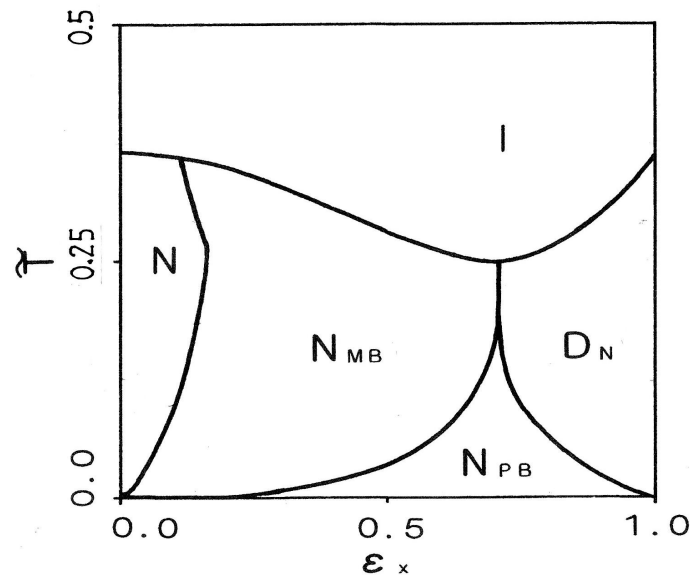


**Figure 1.** Phase diagram on the plane of temperature versus the form factor,  $\epsilon_x$ . The temperature is normalized as  $\tilde{T} \equiv k_B T / u$ , and form factor  $\epsilon_x$  is changed from zero to 1, with  $\epsilon_y$  being kept zero. This figure is based on figure 2 in Hosino, M. & Nakano, H. [13], although with a revised temperature scale.

In this article, the phase diagram on the plane of the anisotropy parameter  $\epsilon_x$  versus temperature, with  $\epsilon_y$  vanishing, is shown (Fig. 1).  $\epsilon_x$ , and  $\epsilon_y$  are the parameters representing the anisotropy of, respectively, the x-direction and y-direction of molecule toward its z-direction. They had already defined in our previous paper [13]. Here, only the isotropic phase I and the nematic phase N appear in the case where  $\epsilon_x = 0$ , while, only the isotropic phase I and the disco-nematic phase  $D_N$  appear in the case where  $\epsilon_x = 1$ . Hereafter, the isotropic, nematic, and the disco-nematic phases are abbreviated symbolically to I, N, and  $D_N$  phase, respectively.

In the case where  $0 < \epsilon_x < 1$ , we have the nematic phase N, two sorts of biaxial nematic phases, and the disco-nematic phase  $D_N$ , as the ordered phases displayed by the system. The two biaxial nematic phases was been divided each other by Priest and Lubensky [15], who named them the molecular-biaxial phase  $N_{MB}$  and phase-biaxial phase  $N_{PB}$ , respectively. It is shown that the disco-nematic phase does not appear in the region where the value of  $\epsilon_x$  is smaller than 0.705 and that the nematic phase does not appear in the region where the value of  $\epsilon_x$  is larger than 0.705. That is, the value  $\epsilon_x = 0.705$  is a boundary which separates the region where the phases for the assembly of biaxial, rod-like molecules appear (abbreviated to ‘rod-like region’) from that where the phases for the assembly of biaxial, disc-like molecules appear (abbreviated to ‘disc-like region’).

One of the present authors also carried out an investigation based on the assembly of molecules with a hard-core of rectangular parallelepipeds having length  $L$ , breadth  $B$ , and depth  $D$ , and the results, which is similar to those achieved by the assembly of molecules in a pair-wise manner via dispersive force, was obtained [16]. Notably, we also confirmed the presence of a “self-dual” condition, as given by Straley. That is, the value  $B / D = 2.237$ , where  $L / D = 5.0$ , and 3.10 where  $L / D = 10.0$  constitute the boundary values that divides the rod-like region from the disc-like region. These values are consistent with the “self-dual” condition given by Straley.

Subsequently, one of the present authors investigated the chiral phases in the assembly of biaxial molecules. As a result, the intermolecular potential energy due to the dispersion force between the induced dipole and the induced quadrupole of the electrically neutral molecules was added to that caused by the dispersion force between the induced dipoles of the electrically neutral molecules. To obtain the expression of the term that depends on the dispersion force between the induced dipole and the induced quadrupole of the electrically

neutral molecules, we assume that the molecules have three, mutually orthogonal mirror planes, with inversion symmetry [4]. All cholesteric (abbreviated symbolically as Ch or N\*), chiral molecular-biaxial nematic (abbreviated symbolically as N<sub>MB</sub>\*), chiral phase-biaxial nematic (abbreviated symbolically as N<sub>PB</sub>\*), and chiral discotic (abbreviated symbolically as DCh or D<sub>N</sub>\*) phases appear in the assembly of chiral biaxial molecules. In particular, we showed that the temperature dependence of cholesteric pitch appeared through the temperature dependence of biaxial ordering parameters.

In the previous work, we assumed that the direction of orientational ordering of the molecular long axis (hereafter denoted as the unit vector  $\vec{n}_1$ ) was perpendicular to the axis of the helical structure (hereafter denoted as the unit vector  $\vec{n}_h$ ), around which the direction of orientational ordering of the molecular long axis helically rotated. However, in the present investigation, we assume that the angle between  $\vec{n}_1$  and  $\vec{n}_h$  is some arbitrary value between zero and  $\pi/2$ , in order to make clear the chiral phases in the biaxial molecule assembly. Under this assumption, the obtained free energy of the system depends on the value of this angle, and we determine the equilibrium value of this angle based on this free energy.

In the present article, we restrict the investigation to the rod-like region, for ease of calculation. Three chiral phases appear in this region. One of them is the ordinary cholesteric phase, where the word “ordinary” means that this phase is uniaxial. The direction of  $\vec{n}_1$  rotates spirally along the direction perpendicular to  $\vec{n}_1$  in this phase. The second chiral phase is a biaxial cholesteric phase BCh, which has the orientational ordering of molecular planes around  $\vec{n}_1$ , and where the direction of  $\vec{n}_1$  rotates spirally along the direction of orientational ordering of molecular plane normal (hereafter denoted as the unit vector  $\vec{n}_3$ ). The last one is a new chiral phase, where the direction of  $\vec{n}_3$  spirally rotates along the one of  $\vec{n}_1$ . This phase is now named as 2<sup>nd</sup> chiral phase-biaxial nematic N<sub>PB</sub><sup>2\*</sup>. (Biaxial cholesteric phase is similarly named as 1<sup>st</sup> chiral phase-biaxial nematic N<sub>PB</sub><sup>1\*</sup>.) We also show the possibility of one more chiral phase, where the direction of  $\vec{n}_1$  is declined from the one of  $\vec{n}_h$  and spirally rotates along the one of  $\vec{n}_h$ . This phase is likely to be one called as a

twist-bend nematic(NTB) phase [17].

In this paper, the order variables representing the orientation of the biaxial molecule, the molecular interaction expressed with these order variables, and the free energy of the system obtained, using the symmetry breaking potential method [18,19] are shown in Section 2, and the results obtained, basing on this system's free energy are shown in Section 3. Finally, the conclusions in present study is explained Section 4.

## 2. Order variables, molecular interaction, and system free energy

To investigate the intermolecular potential energy, we define the following tensor, in accordance with Priest and Lubensky [15], for the  $I$ -th molecule:

$$Q_{pq}^{ij}(I) = a_p^i(I)a_q^j(I) - \frac{1}{3}\delta_{pq}\delta_{ij} \quad (p, q = 1, 2, 3; i, j = x, y, z) \quad (1)$$

where  $a_p^i(I)$  denotes the orthogonal component of the unit vector,  $\vec{a}_p(I)$ , parallel to the  $p$ -th principal axis of the  $I$ -th molecule, and  $\delta_{pq}$  and  $\delta_{ij}$  are Kronecker's delta symbols.

**Table I.** Direction cosines between the molecular and laboratory frames

	$x$	$y$	$z$
$\xi$	$\cos\theta\cos\varphi\cos\psi - \sin\varphi\sin\psi$	$\cos\theta\sin\varphi\cos\psi + \cos\varphi\sin\psi$	$-\sin\theta\cos\psi$
$\eta$	$-\cos\theta\cos\varphi\sin\psi - \sin\varphi\cos\psi$	$-\cos\theta\sin\varphi\sin\psi + \cos\varphi\cos\psi$	$\sin\theta\sin\psi$
$\zeta$	$\sin\theta\cos\varphi$	$\sin\theta\sin\varphi$	$\cos\theta$

( $\xi, \eta, \zeta$ ): coordinate axes in the molecular reference frame.

( $x, y, z$ ): coordinate axes in the laboratory reference frame.

**Table II.** Euler angles and order variables of the six possible configurations

$\Omega_n$	$\theta_n$	$\phi_n$	$\psi_n$	$\hat{\sigma}_1$	$\hat{\sigma}_2$	$\hat{\sigma}_3$	$\hat{\sigma}_4$	$\hat{\sigma}_4'$
$\Omega_1$	0	0	0	1	0	0	1/2	1/2
$\Omega_2$	0	0	$\pi/2$	1	0	0	-1/2	-1/2

$\Omega_3$	$\pi/2$	0	0	-1/2	1	3/2	0	1/4
$\Omega_4$	$\pi/2$	0	$\pi/2$	-1/2	1	-3/2	0	-1/4
$\Omega_5$	$\pi/2$	$\pi/2$	0	-1/2	-1	3/2	0	1/4
$\Omega_6$	$\pi/2$	$\pi/2$	$\pi/2$	-1/2	-1	-3/2	0	-1/4

Table I shows the interrelation between the directions of the orthogonal coordinate system ( $\xi, \eta, \zeta$ ) in the molecular frame relative to the orthogonal coordinate system ( $x, y, z$ ) of the laboratory frame, where the direction cosines between the two coordinate systems are shown in terms of the Eulerian angles  $\theta_I, \phi_I, \psi_I$ . As shown in Table II, the orientation of the molecules is restricted to six possible configurations, following Zwanzig [19], who, when discussing the uniaxial nematic phase, used a three-directional model in which the molecule orientations were restricted to three mutually orthogonal directions.

The thermal averages of the orthogonal components of the tensor  $Q_{pq}^{ij}(I)$  are expressed as shown in Eqs. (2) – (5) below:

$$\langle Q_{pq}^{ij}(I) \rangle_0 = 0 \quad (p \neq q), \quad (2)$$

$$\langle Q_{11}^{ij}(I) \rangle_0 = \sigma_1(n_1^i n_1^j - \frac{1}{3}\delta_{ij}) + \frac{1}{2}\sigma_2(n_2^i n_2^j - n_3^i n_3^j), \quad (3)$$

$$\langle Q_{22}^{ij}(I) \rangle_0 = -\frac{(\sigma_1 - \sigma_3)}{2}(n_1^i n_1^j - \frac{\delta_{ij}}{3}) + (\sigma_4' - \frac{\sigma_2}{2})(n_2^i n_2^j - n_3^i n_3^j), \quad (4)$$

$$\langle Q_{33}^{ij}(I) \rangle_0 = -\frac{(\sigma_1 + \sigma_3)}{2}(n_1^i n_1^j - \frac{\delta_{ij}}{3}) - (\sigma_4' + \frac{\sigma_2}{2})(n_2^i n_2^j - n_3^i n_3^j), \quad (5)$$

in terms of the orthogonal  $i$ -component  $n_p^i$  of the unit vector,  $\vec{n}_p$ , which indicates the average direction of the  $p$ -th principal axis. Here,  $\vec{n}_1$  defines the average direction of the long-axis of the molecule. The order parameters  $\sigma_1, \sigma_2, \sigma_3$ , and  $\sigma_4'$  are obtained as thermal averages of the order variables, which are defined in terms of the three Eulerian angles, as shown in Eqs. (6) – (9) below:

$$\hat{\sigma}_1(I) = \frac{3}{2} \cos^2 \theta_I - \frac{1}{2}, \quad (6)$$

$$\hat{\sigma}_2(I) = \sin^2 \theta_I \cos 2\phi_I, \quad (7)$$

$$\hat{\sigma}_3(I) = \frac{3}{2} \sin^2 \theta_I \cos 2\psi_I, \quad (8)$$

$$\hat{\sigma}_4'(I) = \frac{1}{4} (1 + \cos^2 \theta_I) \cos 2\phi_I \cos 2\psi_I, \quad (9)$$

and whose thermal averages (Eqs.(10) and (11)) constitute the order parameters of the system.

$$\sigma_s = \langle \hat{\sigma}_s(I) \rangle_0, \quad (s = 1, 2, 3), \quad (10)$$

$$\sigma_4' = \langle \hat{\sigma}_4'(I) \rangle_0 \quad (11)$$

In Eqs. (2) – (5), (10), and (11), the angular brackets with suffix zero denote that the average value is taken at thermal equilibrium. For convenience,  $\hat{\sigma}_4(I)$ , which is defined later in Eq. (20), is substituted for  $\hat{\sigma}_4'(I)$ . The types of structures indicated with these order parameters shall be shown later in Table III based on the free energy determined in a previous study [13].

**Table III.** Phases characterized by four order parameters and their symbols

Name of the phase	$\sigma_1$	$\sigma_2$	$\sigma_3$	$\sigma_4$	Symbol
Isotropic	0	0	0	0	I
Nematic	finite	0	0	0	N
Molecular biaxial nematic	finite	0	finite	0	N <sub>MB</sub>
Phase-biaxial nematic (y)	finite	finite	finite	finite	N <sub>PB</sub>
/ Phase-biaxial nematic (x)	/ finite (+)	/ 0	/ 0	/ finite (-)	
Discotic (y)	finite	finite	finite	finite	D <sub>N</sub>
/ Discotic (z)	/ finite (-)	/ 0	/ finite (-)	/ 0	

The molecular plate's normal vector is assumed to be oriented along the y-axis. By replacing the y-axis with the z-axis, we can distinguish between the N<sub>PB</sub> and D<sub>N</sub> phases. In the D<sub>N</sub> case, both  $\sigma_2$  and  $\sigma_4$



vanish, with  $\sigma_1$  and  $\sigma_3$  being finite and negative (shown as “finite (-)” in the last row). In contrast, for  $N_{PB}$ , all the order parameters are finite and positive. In the last row, the notation “Discotic ( $\alpha$ )” means that the normal to the molecular plane is along the  $\alpha$ -axis. By replacing the  $y$ -axis with the  $x$ -axis, we can also distinguish the  $N_{PB}$  phase. In this case,  $\sigma_1$  is almost equal to 1, and  $\sigma_4$  is finite and negative, while  $\sigma_2$  and

$\sigma_3$  are both zero. In the fifth row, the notation “Phase-biaxial nematic ( $\beta$ )” means that the molecular plane’s normal vector is aligned along the  $\beta$ -axis.

In the multipole expansion of intermolecular potential, we can assume that the centers of mass of each biaxial molecule randomly distribute through the whole system space, and that molecules have three mutually orthogonal mirror planes with inversion symmetry. We may then write both the induced dipole – dipole interaction potential, and the additional induced dipole – quadrupole interaction potential, between biaxial molecules, as shown in Eq. (12).

$$\begin{aligned}
\Phi_{IJ} = & -U_1(r_{IJ}) \sum_{i=x,y,z} \sum_{j=x,y,z} Q_{11}^{ij}(I) Q_{11}^{ij}(J) \\
& -U_2(r_{IJ}) \sum_{i=x,y,z} \sum_{j=x,y,z} \{Q_{11}^{ij}(I) R^{ij}(J) + R^{ij}(I) Q_{11}^{ij}(J)\} \\
& -U_3(r_{IJ}) \sum_{i=x,y,z} \sum_{j=x,y,z} R^{ij}(I) R^{ij}(J) \\
& -K_1(r_{IJ}) y_{IJ} \sum_{\beta=x,y,z} \sum_{\gamma=x,y,z} \sum_{\alpha=x,y,z} \epsilon_{y\beta\gamma} Q_{11}^{\alpha\beta}(I) Q_{11}^{\alpha\gamma}(J) \\
& -K_{21}(r_{IJ}) y_{IJ} \sum_{\beta=x,y,z} \sum_{\gamma=x,y,z} \sum_{\alpha=x,y,z} \epsilon_{y\beta\gamma} Q_{11}^{\alpha\beta}(I) R^{\alpha\gamma}(J) \\
& -K_{22}(r_{IJ}) y_{IJ} \sum_{\beta=x,y,z} \sum_{\gamma=x,y,z} \sum_{\alpha=x,y,z} \epsilon_{y\beta\gamma} R^{\alpha\beta}(I) Q_{11}^{\alpha\gamma}(J) \\
& -K_3(r_{IJ}) y_{IJ} \sum_{\beta=x,y,z} \sum_{\gamma=x,y,z} \sum_{\alpha=x,y,z} \epsilon_{y\beta\gamma} R^{\alpha\beta}(I) R^{\alpha\gamma}(J)
\end{aligned} \tag{12}$$

In Eq. (12), we have defined

$$R^{ij}(I) \equiv Q_{22}^{ij}(I) - Q_{33}^{ij}(I) \quad (13)$$

and the potentials  $U_1(r_{IJ})$ ,  $U_2(r_{IJ})$ ,  $U_3(r_{IJ})$ ,  $K_1(r_{IJ})$ ,  $K_{21}(r_{IJ})$ ,  $K_{22}(r_{IJ})$ ,

and  $K_3(r_{IJ})$  are functions of the distance  $r_{IJ}$  between the pair of molecules. In Eq. (12), we have assumed that the molecular long-axis ordering direction rotates helically along the y-axis. It should also be noted that, in general,  $K_{21}(r_{IJ}) \neq K_{22}(r_{IJ})$ .

Although both van der Meer and Vertogen [21], and Priest and Lubensky [15] had already proposed interactions between biaxial molecules similar to that expressed in Eq. (12), their models did not completely account for these interactions. The interaction potential proposed by van der Meer and Vertogen included only the  $\hat{\sigma}_1(I)$  and  $\hat{\sigma}_3(I)$  terms, from among all the order variables  $\hat{\sigma}_i(I)$  ( $i = 1, 2, 3, 4$ ) [21], while the potential proposed by Priest and Lubensky only included some of the terms expressed in Eq. (12) [15]. Consequently, their theories were not appropriate for discussing biaxial liquid crystalline phases at all. In previous work, we had also proposed a potential similar to that expressed in Eq. (12), which included only some of the terms from the induced dipole – quadrupole interaction [22]. The potential proposed there was also unsuited for a discussion of the chirality of biaxial liquid crystalline phases. Here, the interaction potential between biaxial molecules proposed in this work is complete, and thus appropriate for discussing the chirality of biaxial liquid crystal phases.

To investigate the long-range orderings in a system of  $N$  biaxial molecules, we apply the symmetry-breaking potential method, using  $\eta_s \hat{\sigma}_s(I)$  as the potential for the orderings  $s = 1, 2, 3$ , and 4, respectively. We will exclude the detailed calculations needed to obtaining the system's free energy, as these have been shown in previous works [4,13,16], focusing simply on the key aspects, and just show the free energy itself.

We must understand the following respect regarding to the unit vector  $\vec{n}_p$ , which indicates the direction of the  $p$ -th principal axis ordering. In an achiral system,  $\vec{n}_p$  is an unchanged vector at all points across the entire space of the system, while in a chiral structure

(i.e., considered in this work as the axis of helical structure lies along the  $y$ -axis), it changes depending on the point  $\vec{r}$  in the system. Thus, in a system which exhibits a chiral structure, if we consider  $(0,1,0)$ ,  $(0,0,1)$ , and  $(1,0,0)$  as  $\vec{n}_p(\vec{r}_I)$  (with  $p = 1, 2, 3$ ), respectively, the following vectors are as shown in Eqs. (14), (15), and (16):

$$\vec{n}_1(\vec{r}_J) = (\sin \Theta \sin(qy_{IJ}), \cos \Theta, \sin \Theta \cos(qy_{IJ})), \quad (14)$$

$$\vec{n}_2(\vec{r}_J) = (\cos \Theta \sin(qy_{IJ}), -\sin \Theta, \cos \Theta \cos(qy_{IJ})), \quad (15)$$

$$\vec{n}_3(\vec{r}_J) = (\cos(qy_{IJ}), 0, -\sin(qy_{IJ})), \quad (16)$$

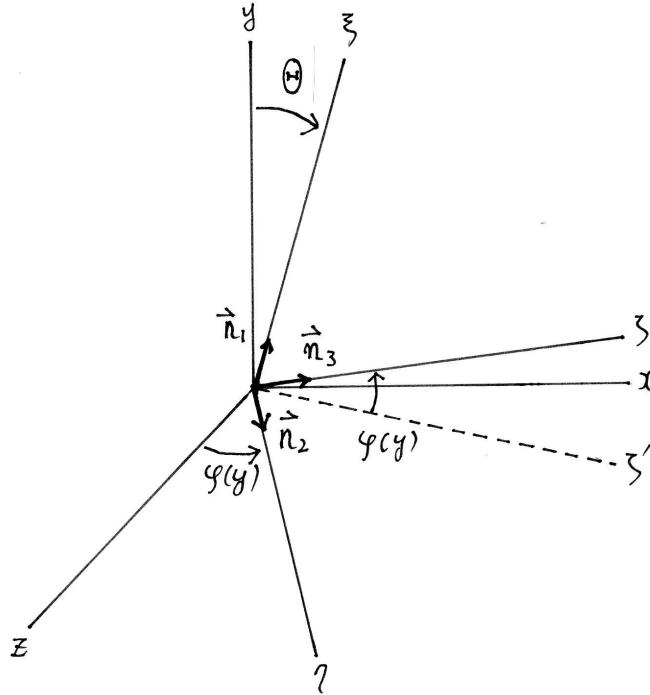


**Figure 2.** The angle  $\Theta$  is that between the direction of the orientational ordering of molecular long axis, which is shown as the  $\xi$ -axis in this Figure, and the axis of the helical structure of the direction of the orientational ordering of the molecular long axis, which is along the  $y$ -axis. The angle  $\phi(y)$  shows the rotation of the  $\xi$ -axis about the  $y$ -axis.

where  $q$  is equal to  $2\pi/p$ , with  $p$  defining the pitch of the chiral structure, and  $y_{IJ}$  as the  $y$  component of the vector joining the centers of the  $I$ -th and  $J$ -th molecules, taken as the

vectors  $\vec{n}_p(\vec{r}_J)$ . (Fig. 2) The present authors deduce molecular interaction expressed in Eq. (12) on the assumption that the helical structure of the molecular long-axis ordering direction lies along the  $y$ -axis. We can then adopt the assumption that  $qy_{IJ}$  is small, in which case, we can expand  $\vec{n}_p(\vec{r}_J)$  as

$$\vec{n}_1(\vec{r}_J) = (0, \cos \Theta, \sin \Theta) + qy_{IJ}(\sin \Theta, 0, 0) - \frac{(qy_{IJ})^2}{2}(0, 0, \sin \Theta), \quad (17)$$

$$\vec{n}_2(\vec{r}_J) = (0, -\sin \Theta, \cos \Theta) + qy_{IJ}(\cos \Theta, 0, 0) - \frac{(qy_{IJ})^2}{2}(0, 0, \cos \Theta), \quad (18)$$

$$\vec{n}_3(\vec{r}_J) = (1, 0, 0) - qy_{IJ}(0, 0, 1) - \frac{(qy_{IJ})^2}{2}(1, 0, 0). \quad (19)$$

Although thermal averages of the orthogonal components of the tensors  $Q_{pq}^{ij}(I)$ ,  $R^{ij}(I)$ ,  $Q_{pq}^{ij}(J)$ , and  $R^{ij}(J)$  are expressed as Eqs. (2) – (5), some caution is necessary; the  $\vec{n}_p$  term appearing in the expressions for  $Q_{pq}^{ij}(I)$  and  $R^{ij}(I)$  is  $\vec{n}_p(\vec{r}_I)$  in Eq. (12), while the term appearing in the expressions for  $Q_{pq}^{ij}(J)$  and  $R^{ij}(J)$  is  $\vec{n}_p(\vec{r}_J)$  in Eq. (12).

Secondly, we adopt the assumptions that the value of  $\sigma_2$  is zero, and that  $\sigma_1$  is some value extremely close to 1, respectively, because we can think that their order parameters might be such values near the  $N_{MB} - N_{PB}$  transition temperature in present case. The orientational ordering of molecular planes around the molecular long axis appears at this transition point, and this ordering parameter affects the behavior of the chiral phases. Then, under this condition, we can make sufficiently clear the behavior of the chiral phase in the rod-like region. Some value extremely close to 1 is used for  $\sigma_1$ , as a parameter in real numerical calculation. Last of all, for ease of calculation, we use  $\hat{\sigma}_4(I)$  defined in Eq. (20), instead of  $\hat{\sigma}'_4(I)$  defined in Eq. (9).

$$\hat{\sigma}_4(I) = \frac{1}{3} \hat{\sigma}'_4(I) (1 + 2\hat{\sigma}_1(I)) = \frac{1}{4} (\cos^2 \theta_I + \cos^4 \theta_I) \cos 2\phi_I \cos 2\psi_I. \quad (20)$$

With these in mind, we finally obtain the free energy of system  $F(\{\sigma_3, \sigma_4\}; q, \Theta)$ , as

$$F(\{\sigma_3, \sigma_4\}; q, \Theta) = F_0 + F_\sigma(\sigma_3, \sigma_4) + \Delta F(\{\sigma_3, \sigma_4\}; q, \Theta), \quad (21)$$

where  $F_0$  is an arbitrary constant, and we have defined the terms  $F_\sigma(\sigma_3, \sigma_4)$  and

$\Delta F(\{\sigma_3, \sigma_4\}; q, \Theta)$  as

$$F_\sigma(\sigma_3, \sigma_4) = \frac{1}{3} \frac{\sigma_3^2}{1 - \sigma_1} + \frac{1}{2} \{ (1 + 2\sigma_4) \ln(1 + 2\sigma_4) + (1 - 2\sigma_4) \ln(1 - 2\sigma_4) \} \\ - \frac{\beta}{2} \left\{ \frac{2}{3} (2U_2^0 \sigma_3 + U_3^0 \sigma_3^2) + 8U_3^0 \sigma_4^2 \right\}, \quad (22)$$

$$\Delta F(\{\sigma_3, \sigma_4\}; q, \Theta) = -\frac{\beta}{2} \{ q (\hat{K}(\sigma_3, \sigma_4) \sin^2 \Theta + 16K_3^1 \sigma_4^2) \\ - q^2 (\hat{U}(\sigma_3, \sigma_4) \sin^2 \Theta + 16U_3^2 \sigma_4^2) \}. \quad (23)$$

We have further defined the terms  $\hat{K}(\sigma_3, \sigma_4)$  and  $\hat{U}(\sigma_3, \sigma_4)$  as

$$\hat{K}(\sigma_3, \sigma_4) = (K_{21}^1 + K_{22}^1) (\sigma_3 + 2\sigma_4) + K_3^1 (\sigma_3 + 2\sigma_4)^2 - 16K_3^1 \sigma_4^2, \quad (24)$$

$$\hat{U}(\sigma_3, \sigma_4) = 2U_2^2 (\sigma_3 + 2\sigma_4) + U_3^2 (\sigma_3 + 2\sigma_4)^2 - 16U_3^2 \sigma_4^2, \quad (25)$$

which are given in terms of the integrals as shown in Eqs. (26) – (29):

$$U_n^0 = \frac{4\pi}{3} \rho \int r^2 U_n(r) dr, (n = 1, 2, 3), \quad (26)$$

$$U_n^2 = \frac{4\pi}{3} \rho \int r^4 U_n(r) dr, (n = 1, 2, 3), \quad (27)$$

$$K_n^0 = \frac{4\pi}{9} \rho \int r^2 K_n(r) dr, (n = 1, 2, 3), \quad (28)$$

$$K_n^1 = \frac{4\pi}{9} \rho \int r^3 K_n(r) dr. (n = 1, 2, 3). \quad (29)$$

To determine the minimum free energy value of Eq. (21), with respect to the order parameters,  $\sigma_s$  ( $s = 3, 4$ ), the equilibrium configuration is defined, based on the requirement that

$$\frac{\partial F(\sigma_1, \sigma_2, \sigma_3, \sigma_4)}{\partial \sigma_s} = \frac{\partial F_\sigma(\sigma_3, \sigma_4)}{\partial \sigma_s} = 0. (s = 3, 4) \quad (30)$$

Terms in Eq. (21) which are proportional to  $q$  and  $q^2$  are neglected when the order parameters equilibrium values are determined using Eq. (30), given that we have considered  $q$  to be small, and thus the terms which include them do not greatly influence the equilibrium values of the order parameters. We can divide Eq. (30) into two equations, with respect as  $\sigma_3$  and  $\sigma_4$ , since the term including both  $\sigma_3$  and  $\sigma_4$  is not in  $F_\sigma$ . Therefore, the calculations

determining the minimum free energy value with respect to order parameters become easier.

The equilibrium value of  $q$ ,  $\Theta$  is determined using the equilibrium values of the order parameters, based on the requirements

$$\frac{\partial \Delta F(\bar{\sigma}_3, \bar{\sigma}_4 : q, \Theta)}{\partial q} = 0, \quad (31)$$

and

$$\frac{\partial \Delta F(\bar{\sigma}_3, \bar{\sigma}_4 : q, \Theta)}{\partial \Theta} = 0, \quad (32)$$

which minimize the free energy of Eq. (21) with respect to  $q$ , and  $\Theta$ , respectively.  $\bar{x}$  in Eqs. (31) and (32) denotes the equilibrium value of the quantity  $x$ . Then, we can obtain the equilibrium value of  $q$  with Eq. (31) as

$$\bar{q} = \frac{1}{2} \frac{\hat{K}(\bar{\sigma}_3, \bar{\sigma}_4) \sin^2 \bar{\Theta} + 16 K_3^1 \bar{\sigma}_4^2}{\hat{U}(\bar{\sigma}_3, \bar{\sigma}_4) \sin^2 \bar{\Theta} + 16 \mathcal{U}_3^2 \bar{\sigma}_4^2}, \quad (33)$$

and the following equation, with the equilibrium condition with respect to  $\Theta$  with Eq. (32) as:

$$2\bar{q} \sin \bar{\Theta} \cos \bar{\Theta} (\hat{K}(\bar{\sigma}_3, \bar{\sigma}_4) - \bar{q} \hat{U}(\bar{\sigma}_3, \bar{\sigma}_4)) = 0. \quad (34)$$

This equation gives four solutions as ( i )  $\bar{q} = 0$ , ( ii )  $\cos \bar{\Theta} = 0$ , ( iii )  $\sin \bar{\Theta} = 0$ , ( iv )  $\hat{K}(\bar{\sigma}_3, \bar{\sigma}_4) - \bar{q} \hat{U}(\bar{\sigma}_3, \bar{\sigma}_4) = 0$ . In case ( i ), the solution is trivial, and is hereafter excluded from the discussion, as the excessive energy,  $\Delta F$ , is identical to zero, and it is thought that no information is obtained based on  $\Delta F$ . In case ( ii ), the orientational configuration is similar to that for the cholesteric phase. In case ( iii ), the direction of the orientational ordering of the molecular long axis,  $\vec{n}_1$ , is parallel to the axis of the helical structure,  $\vec{n}_h$ , and it is shown in the following that the direction of the orientational ordering of the molecular plane normal  $\vec{n}_3$ , instead of  $\vec{n}_1$ , helically rotates along  $\vec{n}_h$ , if the orientational ordering of the molecular plane appears in this phase. Therefore, we can name this new chiral

phase as a 2<sup>nd</sup> chiral phase-biaxial phase (abbreviated symbolically as N<sub>PB</sub><sup>2\*</sup>). Finally, in case (iv), the orientational configuration is similar to that for the twist-bend nematic (NTB) phase.

Based on two equations: Eq. (30),  $\hat{K}(\bar{\sigma}_3, \bar{\sigma}_4) - \bar{q}\hat{U}(\bar{\sigma}_3, \bar{\sigma}_4) = 0$ , we can determine the equilibrium value of  $\sin^2 \Theta$ . It is necessary to verify whether this value exists in the region from zero to 1. If the value of  $\sin^2 \Theta$  exists in this region, we can consider that NTB phase is able to appear in the present system (Fig. 3).

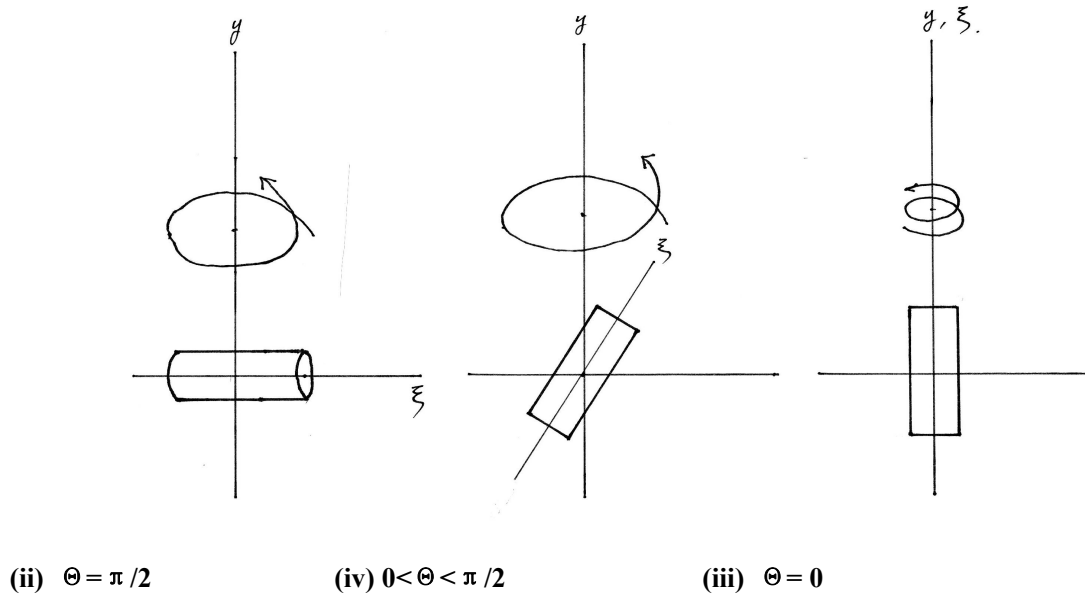


**Figure 3.** Cases (ii), (iv), and (iii) shows cholesteric, twist-bend nematic, and 2<sup>nd</sup> chiral phase-biaxial nematic phases, respectively, with 2<sup>nd</sup> chiral phase-biaxial nematic phase named for the first time in the present article.

Using the equilibrium value of the excessive energy,  $\Delta F$ , we can determine which phase appears in the system at each temperature. In the following section, we obtain numerically the free energy of the present system, showing the results obtained from these calculations.

### 3. Results based on a model for the molecular dipole and quadrupole polarization

To begin the calculations, we need to investigate the relationship between the interaction potentials,  $U_1$ ,  $U_2$ , and  $U_3$ , and those between the interaction potentials,  $K_1$ ,  $K_{21}$ ,  $K_{22}$ , and  $K_3$ ,



in Eq. (12). These have been previously investigated [4, 13] by assuming a simple model of the molecule's transition dipole and transition quadrupole moments and we can write the ratios of  $U_2^0$  and  $U_3^0$  to  $U_1^0$ , of  $U_2^2$  and  $U_3^2$  to  $U_1^2$ , and those of  $K_{21}^n$ ,  $K_{22}^n$ , and  $K_3^n$  to  $K_1^n$  ( $n = 0, 1$ ), as shown in Eqs. (35) and (36):

$$\frac{U_2^n}{U_1^n} = \alpha, \quad \frac{U_3^n}{U_1^n} = \alpha^2, \quad (n = 0, 2) \quad (35)$$

$$\frac{K_{21}^n}{K_1^n} = \alpha, \quad \frac{K_{22}^n}{K_1^n} = -\frac{1}{3\alpha}, \quad \frac{K_3^n}{K_1^n} = -\frac{1}{3} \quad (n = 0, 1) \quad (36)$$

where the parameter  $\alpha$  represent the shape of the molecule defined as shown in Eq. (37):

$$\alpha \equiv \frac{\varepsilon_x^2 - \varepsilon_y^2}{2 - (\varepsilon_x^2 + \varepsilon_y^2)}. \quad (37)$$

The results of our calculation depend on the reduced temperature and the reduced pitch terms, defined as

$$\tilde{T} = \frac{k_B T}{U_1^0}, \quad (38)$$

$$\tilde{q} = \frac{\bar{q}}{q_0} = \bar{q} R \left/ \frac{K_1^0}{U_1^0} \right. . \quad (39)$$

In the following, the reduced free energy defined in Eq. (40), is also used.

$$\tilde{F} = \frac{\Delta F}{(K_1^0/U_1^0)^2}. \quad (40)$$

As we have used the reduced temperature and the reduced pitch in our calculations up to now, the free energy expressed in Eq. (21) only depends on the molecular shape through the shape factor  $\alpha$ , and the reduced pitch is determined

$$\tilde{q} = \frac{1}{2} \frac{\widehat{K}(\bar{\sigma}_3, \bar{\sigma}_4) \sin^2 \bar{\Theta} + 16 K_3^1 \bar{\sigma}_4^2}{\widehat{U}(\bar{\sigma}_3, \bar{\sigma}_4) \sin^2 \bar{\Theta} + 16 U_3^2 \bar{\sigma}_4^2}. \quad (41)$$

Numerical calculations were carried out for the anisotropy parameters  $\epsilon_x = 0.2, 0.3, 0.4, 0.5, 0.6, \text{ and } 0.7$ , subject to the condition that  $\epsilon_y = 0.0$ . Each case corresponds to the value,  $\alpha = 0.0204, 0.0421, 0.0870, 0.1429, 0.2195, \text{ and } 0.3245$ , respectively. Definitions of  $\epsilon_x$ ,  $\epsilon_y$ , and  $\alpha$  have been given previously [13]. In these cases, the assumption regarding values for  $\sigma_2$  and  $\sigma_1$  is adequate, especially near the  $N_{MB} - N_{PB}$  transition temperature,  $\tilde{T}_{MP}$ . We show the results in Fig. 4. The  $N_{MB} - N_{PB}$  transition, where the order parameter,  $\sigma_4$  changes from zero to a positive value, occurs in each case by decreasing the temperature. The order parameter,  $\sigma_4$  represents the rotating distribution of molecular planes around the molecular long axis, with the direction of orientational ordering of the molecular plane normal apparently denoted by the unit vector  $\vec{n}_3$ .

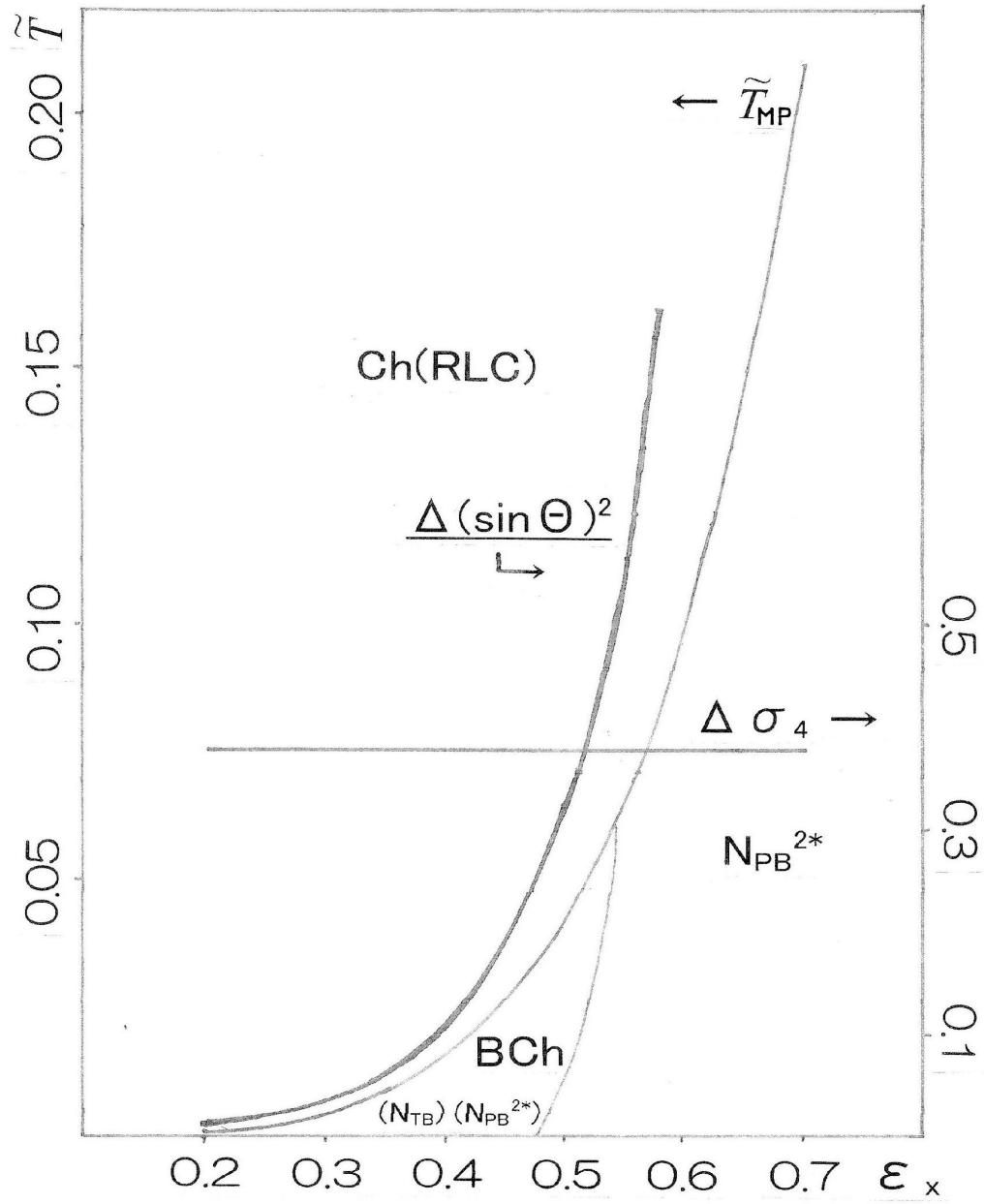


**Figure 4.** Temperature versus anisotropy factor  $\epsilon_x$  phase diagram. Temperature is reduced, as shown in Eq. (38), and the changes to  $\sigma_4$  and  $(\sin \Theta)^2$  at the transition temperature are shown here. Symbols:  $(N_{TB})$  and  $(N_{PB}^{2*})$  indicate that the orientational configurations corresponding to NTB and  $N_{PB}^{2*}$  phases are the solutions of Eq. (34), in this region.

In cases where  $\varepsilon_x = 0.2, 0.3, 0.4$ , and  $0.5$ , the phase that appears in a system of molecules at a temperature higher than  $\tilde{T}_{MP}$  is a cholesteric phase. The normals of the molecular plane distribute uniformly around the molecular long axis in this phase. While the phase that appears at temperature lower than  $\tilde{T}_{MP}$  is a cholesteric phase, as  $\Theta$  is  $\pi/2$ , although  $\sigma_4$  is positive and finite. The orientational ordering of the molecular plane appears and the direction of this orientational ordering of the molecular plane normal  $\vec{n}_3$ , is parallel to  $\vec{n}_h$ , in this phase. We name this phase as a biaxial cholesteric (abbreviated symbolically as BCh) phase or 1<sup>st</sup> chiral phase-biaxial nematic phase (abbreviated symbolically as N<sub>PB</sub><sup>1\*</sup>). Furthermore, the solutions of Eq. (34) corresponding to the orientational configurations similar to those in the NTB phase and in N<sub>PB</sub><sup>2\*</sup> one exist at temperature lower than  $\tilde{T}_{MP}$ , but the phases having these orientational configurations do not appear, since the energies of these phases are greater than that of the BCh phase.

In cases where  $\varepsilon_x = 0.6$ , or  $0.7$ , the phase that appears at temperature higher than  $\tilde{T}_{MP}$  is also a Ch phase, which does not have the orientational ordering of the molecular plane, although the N<sub>PB</sub><sup>2\*</sup> phase appears at temperature lower than  $\tilde{T}_{MP}$ . However, the solution of Eq. (34) corresponding to the orientational configuration in the NTB phase does not appear at any temperature lower than  $\tilde{T}_{MP}$ .

By additional calculation in the case where the value of  $\varepsilon_x$  exists between  $0.5$  and  $0.6$ , it is made clear that there are two types of helical structure in the phase where  $\sigma_4$  is finite. The one is a helical structure of  $\vec{n}_1$  (hereafter this is called as a rod-like helix), and another one is one of  $\vec{n}_3$  (hereafter this is called as a disc-like one). Furthermore, the transition from a phase with rod-like helix to one with disc-like helix occurs as decreasing temperature, although no order parameter indicates this transition point. (Fig. 1) This result suggests how the difference between a ordinary cholesteric phase and a disco-cholesteric one occurs, depending on the molecular shape and / or the anisotropy of molecular interaction. We shall discuss this point in detail in the following section.

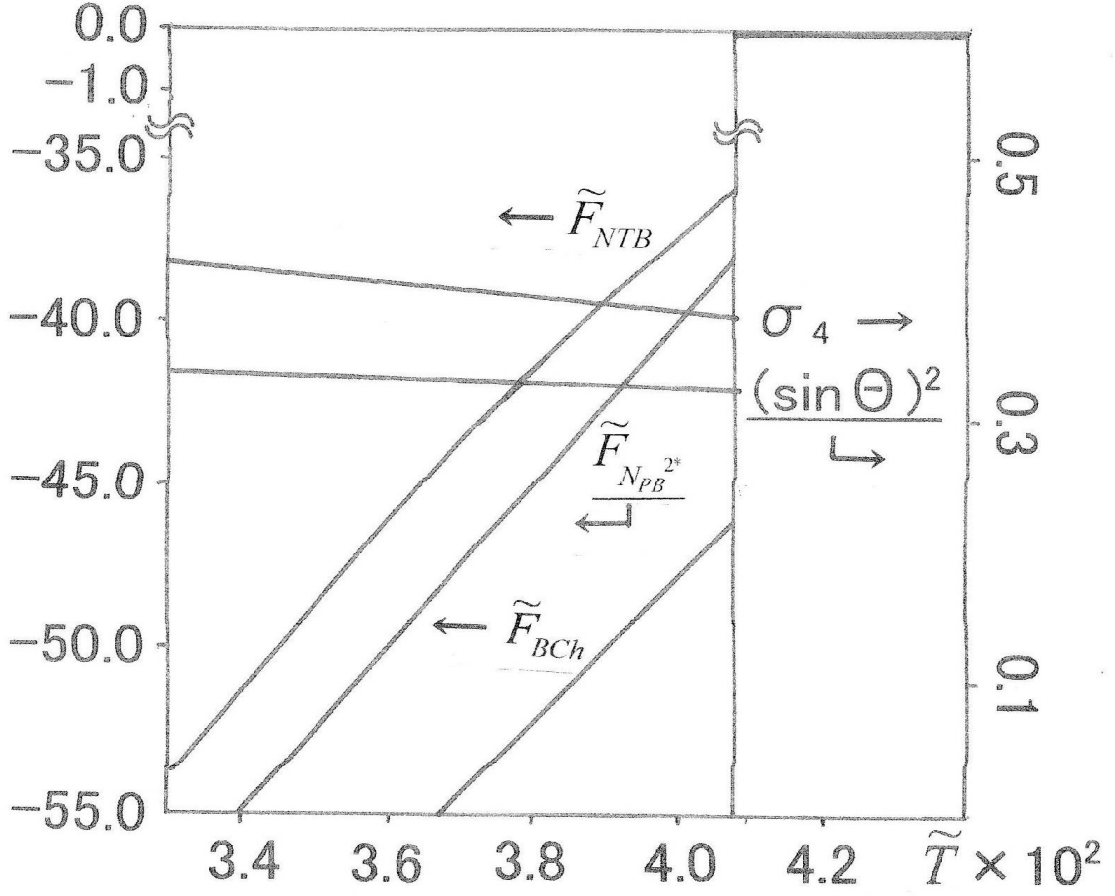


**Figure 5.** Temperature dependence of the order parameter,  $\sigma_4$ ,  $(\sin \Theta)^2$ , the free energy of the biaxial cholesteric phase,  $\tilde{F}_{BCh}$ , one of the NTB phase,  $\tilde{F}_{NTB}$ , and one of the  $N_{PB}^{2*}$  phase,  $\tilde{F}_{N_{PB}^{2*}}$ , in the case where  $\epsilon_x = 0.5$ , as deduced in Eq. (40), are shown here. At a temperature above  $\tilde{T}_{MP}$ ,  $\tilde{F}_{N_{PB}^{2*}}$  and  $\tilde{F}_{NTB}$  equal zero, and while,  $\tilde{F}_{BCh}$  does not equal zero, although its magnitude is too small to show on this figure.

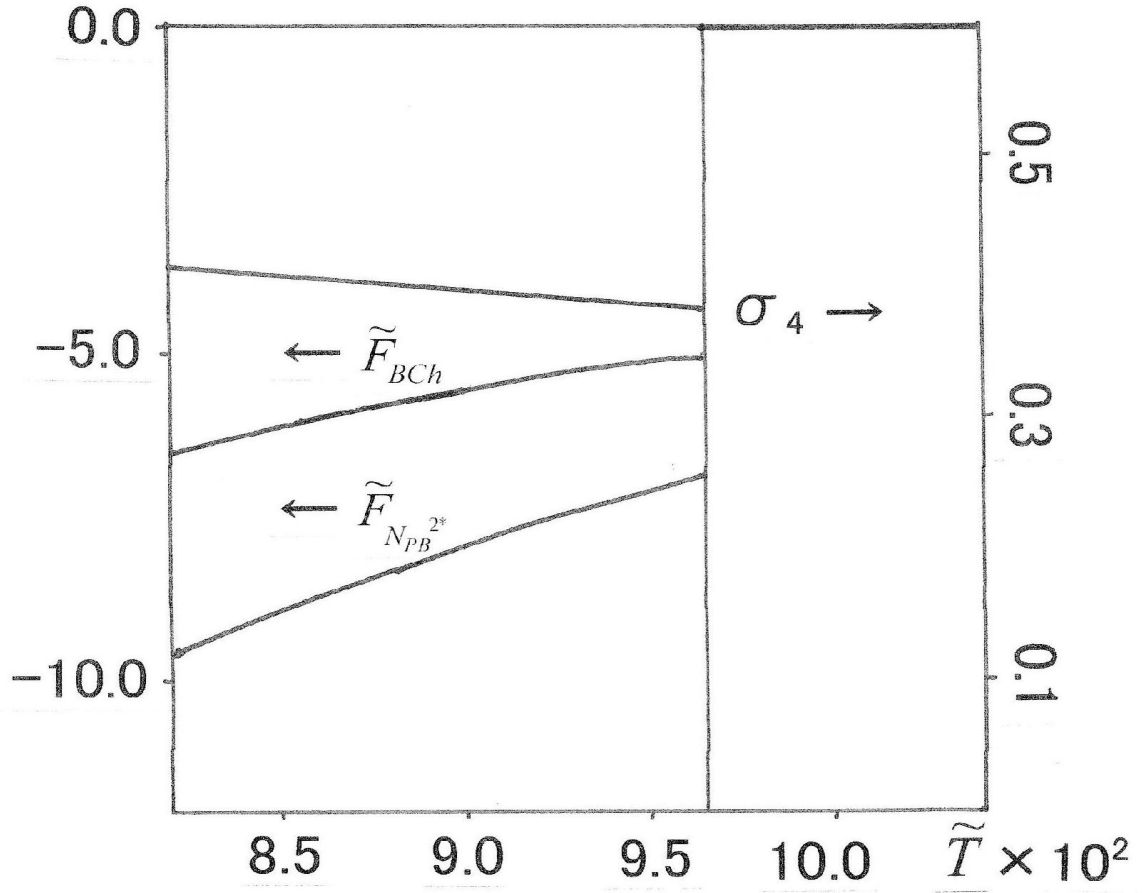


**Figure 6.** Temperature dependence of the order parameter,  $\sigma_4$ , the free energy of the biaxial cholesteric phase,  $\tilde{F}_{BCh}$ , and one of the 2<sup>nd</sup> chiral phase-biaxial nematic phase,  $\tilde{F}_{NPB^{2*}}$ , for the case where  $\epsilon_x = 0.6$ , and as deduced in Eq. (40), are shown here. At temperatures above the transition,  $\tilde{F}_{NPB^{2*}}$  is equal to zero, and while  $\tilde{F}_{BCh}$  is not equal to zero, although it is too small to show in this figure.

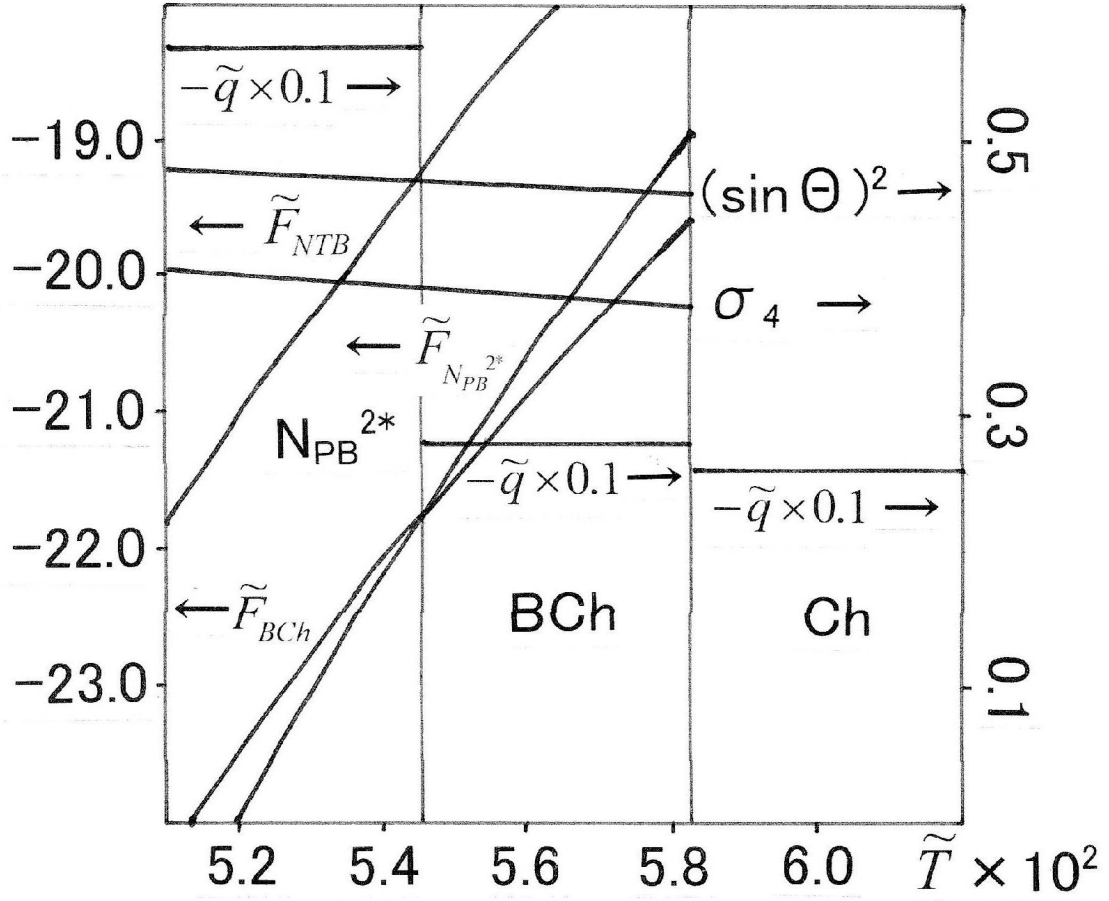


**Figure 7.** Temperature dependence of the order parameter,  $\sigma_4$ ,  $(\sin \Theta)^2$ , the deduced pitch,  $\tilde{q}$ , defined in Eq. (39), the free energy of the biaxial cholesteric phase,  $\tilde{F}_{BCh}$ , one of the 2<sup>nd</sup> chiral phase-biaxial nematic phase,  $\tilde{F}_{N_{PB}^{2*}}$ , and one of the twist-bend nematic phase,  $\tilde{F}_{NTB}$ , for the case where  $\epsilon_x = 0.54$ , and as deduced in Eq. (40), are shown here. At higher temperatures than  $\tilde{T}_{MP}$ ,  $\tilde{F}_{N_{PB}^{2*}}$  and  $\tilde{F}_{NTB}$  are equal to zero, and while the value of  $\tilde{F}_{BCh}$  is between 0 and -0.60 and is not shown in this figure.  $\tilde{q}$  does not scarcely depend on temperature, although it changes at  $\tilde{T}_{MP}$  and BCh- $N_{PB}^{2*}$  transition temperatures.

The temperature dependence of the order parameter,  $\sigma_4$ ,  $(\sin \Theta)^2$ , the free energy of the BCh phase,  $\tilde{F}_{BCh}$ , one of the NTB phases,  $\tilde{F}_{NTB}$ , and one of the  $N_{PB}^{2*}$  phase,  $\tilde{F}_{N_{PB}^{2*}}$  are shown in Figs 5 (for the case where  $\epsilon_x = 0.5$ ) and 6 (for the case where  $\epsilon_x = 0.6$ ). As decreasing temperature in  $N_{PB}$  phase, the order parameter,  $\sigma_4$  increases slightly, and  $(\sin \Theta)^2$  decreases slightly. In the case where  $\epsilon_x = 0.5$ , at the temperature lower than  $\tilde{T}_{MP}$ , both  $\tilde{F}_{N_{PB}^{2*}}$  and  $\tilde{F}_{NTB}$  are certainly larger than  $\tilde{F}_{BCh}$ , and  $\tilde{F}_{NTB}$  is also larger than  $\tilde{F}_{N_{PB}^{2*}}$ .

In the case where  $\epsilon_x = 0.5$ , the value of  $\tilde{q}$  changes from -3.834 to -4.058 at  $\tilde{T}_{MP}$ , as decreasing temperature of the system, but  $\tilde{q}$  does not depend so much on temperature. Temperature dependence of  $\tilde{q}$  at lower temperature than  $\tilde{T}_{MP}$  is slightly larger than one at higher temperature than  $\tilde{T}_{MP}$ . In the case where  $\epsilon_x = 0.6$ , the value of  $\tilde{q}$  changes from -1.480 to -3.459 at  $\tilde{T}_{MP}$ , as decreasing temperature of the system, but  $\tilde{q}$  does not depend so much on temperature. In the case where  $\epsilon_x = 0.54$ , the value of  $\tilde{q}$  firstly changes from -2.618 to -2.808 at  $\tilde{T}_{MP}$ , and secondly changes from -2.813 to -5.721 at the transition temperature from BCh phase to  $N_{PB}^{2*}$  one, as decreasing temperature of the system, but  $\tilde{q}$  does not depend so much on temperature also in this case. (Fig. 7) It is thought that the change of helix type causes the larger change of the value of  $\tilde{q}$  than one at  $\tilde{T}_{MP}$ .

## 4. Conclusions

We have investigated the chiral phases in the system of chiral biaxial molecules located in the rod-like region and have demonstrated that Ch, BCh, and  $N_{PB}^{2*}$  phases appear in this system. We also concluded that the NTB phase might appear, as the solution to Eq. (34) corresponding to the orientational configuration of the NTB phase exists at lower temperature than  $\tilde{T}_{MP}$ . However, the NTB phase does not appear as an equilibrium state, as the free energy of this phase is larger than that of the other phases.



In  $N_{PB}$  phase, we are able to define two directors,  $\vec{n}_1$ ,  $\vec{n}_3$ , as order parameter  $\sigma_4$  is finite. Therefore, two types of helical structure appear in this phase. One is a rod-like helix and another one is a disc-like one. In the case of rod-like region, as increasing temperature from the temperature where a phase with a rod-like helix exists, the phase transition occurs at  $\tilde{T}_{MP}$ , and  $\sigma_4$  becomes zero, therefore, orientational ordering of molecular plane around long axis of molecule disappears. But, the structure of rod-like helix remains over  $\tilde{T}_{MP}$ , although  $\sigma_4$  becomes zero. Thus, ordinary cholesteric phase appears. When a value of  $\epsilon_x$  is larger than 0.55,  $BCh(N_{PB}^{1*})$  phase does not appear and a direct transition from  $N_{PB}^{2*}$  phase to Cholesteric one occurs, as increasing temperature. But, we can explain similarly the appearance of cholesteric phase, as we can think that a rod-like helix exists at transition temperature if we think that  $N_{PB}^{2*} - BCh(N_{PB}^{1*})$  transition and  $BCh(N_{PB}^{1*}) - Ch$  one occur simultaneously at transition temperature  $\tilde{T}_{MP}$ .

We can assume similar mechanism mentioned above also in the case of disc-like region. In this case, as increasing temperature from the temperature where a phase with a disc-like helix exists, the phase transition occurs at  $\tilde{T}_{MP}$ , and  $\sigma_4$  becomes zero, therefore, orientational ordering of molecular long axis around the normals of molecular plane disappears. However, the structure of disc-like helix remains over  $\tilde{T}_{MP}$ , although  $\sigma_4$  becomes zero. Thus, a chiral disco-nematic( $D_N^*$ ) phase appears. After present investigation, it shall be necessary to study chiral phases in the system of disc-like biaxial molecules. This will be comparatively simple task, and we can expect to report these results soon.

If we introduce the smectic order parameter into present theory, it is able to make clear whether the biaxial phase and the chiral phase with the smectic order exist or not. For example, if NTB phase shown in present article have a smectic order and the normal of smectic layer corresponds with the axis of helix structure of the direction of orientational ordering of molecular long axis, this phase is apparently a smectic  $C^*$  phase. Thus, we can construct the theory of a smectic  $C^*$  phase, introducing a smectic order parameter into present theory. When we carry out such an investigation, it might be needed that the mechanism stabilizing a smectic C phase is introduced into the theory. As an example of such a mechanism, we can refer to the intermolecular potential energy proposed by van der Meer

and Vertogen. This is the permanent dipole – induced dipole interaction potential and explained the appearance of the smectic C phase [24].

## Acknowledgments

We would like to thank Dr. H. Kimura, and Dr. H. Nakano, who have since passed away, for their encouragement and guidance over the years. We would also like to thank Editage ([www.editage.com](http://www.editage.com)) for English language editing.

## References

- [1] van der Meer, B.W. (1979). Doctoral Thesis (in Dutch), Groningen Univ.:Groningen, NED.
- [2] Kimura, H., Hosino, M., & Nakano, H. (1979). J. Phys.(Paris),40,C3–173.
- [3] Kimura, H., Hosino, M., & Nakano, H. (1982). J. Phys. Soc. Jpn, 51, 1584.
- [4] Hosino, M.(2017). Mol. Cryst. Liq. Cryst.,658:1, 92.
- [5] Yu, L.J., & Saupe, A. (1980). Phys. Rev. Lett., 45, 1000.
- [6] Saupe, A., Broonbrahm, P., & Yu, L.J. (1983). J. Chem. Phys., 80, 7.
- [7] Chandrasekhar, S., Sadashiva, B.K., Ramesha, S., & Srikanta, B.S. (1986). Pramana, 27, L713.
- [8] Chandrasekhar, S., Sadashiva, B.K., & Suresh, K.A. (1977). Pramana, 9, 471.
- [9] Beguin, A., Billard, J., Dubois, J.C., Nguyen Huu Tinh, & Zann, A. (1979). J. Phys.(Paris), 40, C3–15.
- [10] Destrade, C., Moncton, M.C., & Malthete, J. (1979). J. Phys. (Paris), 40, C3–17.
- [11] Freiser, M.J. (1970). Phys. Rev. Lett., 24, 1041.
- [12] Straley, J.P. (1974). Phys. Rev. A, 10, 1881.
- [13] Hosino, M. & Nakano, H. (2000). Mol. Cryst. Liq. Cryst.,348:1, 207.
- [14] Sonnet, A.M., Virga, E.G., & Durand, G.E. (2003). Phys. Rev. E, 67, 061701–1.
- [15] Priest, R.G. & Lubensky, T.C.(1974). Phys. Rev. A, 9, 893.
- [16] Hosino, M. (2017). Mol. Cryst. Liq. Cryst.,658:1, 1.
- [17] Borshch, V. et.al. (2013). Nature Commu., 4, 2635.
- [18] Nakano, H. & Hattori, M. (1973). Prog. Theor. Phys., 49, 1752.
- [19] Nakano, H. & Kimura, H. (1988). Statistical Thermodynamics of Phase Transitions (in Japanese), Asakura: Tokyo, JPN.
- [20] Zwanzig, R. J. (1963). Chem. Phys., 39, 1714.
- [21] van der Meer, B.W. & Vertogen, G. (1976). Phys. Lett.,59A, 279.
- [22] Hosino,M. (1981). Doctoral Thesis (in Japanese), Dept. Appl. Phys., Nagoya Univ.:

Nagoya, Japan.

- [23] Fukuda, A. & Takezoe, H. (1990). Structures and Properties of Ferroelectric Liquid Crystals (in Japanese), Corona Publishing Co. Ltd.: Tokyo, JPN.
- [24] van der Meer, B.W. & Vertogen, G. (1979). J. Phys. (Paris), 40, C3–222.